Conference on Modelling Fluid Flow (CMFF'25)
The 19th International Conference on Fluid Flow Technologies
Budapest, Hungary, August 26-August 29, 2025

MODELLING THE METABOLIC AND MYOGENIC CONTROL IN HUMAN BLOOD CIRCULATION

Richárd WÉBER[1], Márta VIHAROS[2], György PAÁL[3]

[1] Department of Hydrodynamic Systems, Faculty of Mechanical Engineering, Budapest University of Technology and Economics. H-1111 Budapest, Műegyetem rkp. 3., Hungary. Corresponding Author, E-mail: rweber@hds.bme.hu
[2] Department of Hydrodynamic Systems, Faculty of Mechanical Engineering, Budapest University of Technology and Economics. H-1111 Budapest, Műegyetem rkp. 3., E-mail: viharos.marti@gmail.com
[3] Department of Hydrodynamic Systems, Faculty of Mechanical Engineering, Budapest University of Technology and Economics. H-1111 Budapest, Műegyetem rkp. 3., E-mail: gypaal@hds.bme.hu

ABSTRACT

Hemodynamics, the study of blood flow dynamics, is a fundamental aspect of cardiovascular physiology, governing the delivery of oxygen and nutrients to tissues. A critical mechanism, ensuring stable blood flow under varying conditions, such as changes in blood pressure, is autoregulation. The myogenic response, a cornerstone of autoregulation, involves the contraction of arterioles in response to increased intravascular pressure, thereby stabilizing blood flow. Similarly, metabolic responses regulate vascular tone in accordance with the metabolic demands of tissues, ensuring an adequate supply of oxygen [1].

This study introduces refined mathematical models of regulatory mechanisms, implemented within a one- and zero-dimensional hemodynamics solver, first_blood[2]. The simulation mimics the body's response to changes by considering the peripheral resistances varying. Simulation results are systematically evaluated against established physiological knowledge. The findings demonstrate that the simulations can reproduce the behaviour of the control mechanisms. Specifically, the myogenic and metabolic response models yielded qualitatively accurate results. Future work will focus on validation with clinical in-vivo measurement data.

Keywords: metabolic control, myogenic control, haemodynamics, one- and zero-dimensional simulations

NOMENCLATURE

C	Oxygen concentration $\left[\frac{m^3}{m^3}\right]$
G	Static gain [1]
R	Vascular resistance $\left[\frac{m^3}{m^3}\right]$
M	Maximum oxygen consumption rate $\left[\frac{m^3(O_2)}{s \cdot m^3(plasma)}\right]$
a	Inner vessel radius $[m]$
b	Outer vessel radius $[m]$
c	A constant parameter $[m^2]$
f	Parameter of a sigmoid curve $\left[\frac{1}{Pa}\right]$ or $\left[\frac{m^3}{m^3}\right]$
k	A constant parameter [1]
u	A constant parameter [1]
p	Pressure $[Pa]$
t	Time $[s]$
x	Independent variable of a sigmoid curve $[Pa]$ or $[s]$
σ_θ	Circumferential wall tension $[Pa]$

Subscripts and Superscripts

fact	Scaling factor
max	Maximal value
met	Metabolic
min	Minimal value
myo	Myogenic

1. INTRODUCTION

The human circulatory system is responsible for transporting viable nutritions, ions, oxygen, etc. to the tissues. Maintaining blood flow and pressure is inevitable to keep the body functional. Although the complexity of blood flow regulation is high, modelling of such phenomena might help in understanding the fundamental operations, in decision-making or diagnose. Besides physiological and hormonal effects, three major control mechanisms influence blood pressure: myogenic, metabolic and neural. While the neural one uses baroreceptors from various locations of the arterial network controlling the heart, the former two are local mechanisms effecting only the diameter of arterioles.

In suboptimal conditions (e.g., low blood pressure or low tissue O_2 (oxygen) levels), the system attempts to correct this through regulation mechanisms that control the amount of blood flowing through the capillaries. Local regulation consists of two main

phenomena: myogenic and metabolic mechanisms that operate indepedently. The former responds to changes in blood pressure, while the latter responds to changes in the chemical composition [1], from which, the study focuses on the O_2 level. This work aims to capture the known and accepted characteristics of these processes. It also applies the O_2 transport modelling, that is also presented at this conference, titled "Modelling the transport of oxygen in the human vascular system".

Arteries are responsible for delivering oxygenated blood to organs and tissues. These vessels vary in diameter and length, with each type serving a different purpose. Smaller arterial vessels include arterioles, terminal arterioles, and capillaries, with diameters of 20-200 μm, 8-20 μm, and 4-7 μm, respectively. Larger arteries have relatively low vascular resistance, contributing about 10% to the total vascular resistance, while small arteries and arterioles contribute 50-55%, capillaries 30-35%, and the rest comes from venules and veins [3].

When considering autoregulation, the brain often comes to mind first, as it is one of the most vital organs in the body. The blood supply to the intracranial system is therefore a high priority, with a numerical value around $50-60\ \frac{\text{ml}}{\text{min}\ 100\ \text{g}}$, around 20% of the cardiac output when the body is at rest [4]. Cerebral autoregulation can be seen as the body's attempt to maintain this value under various conditions. Physicians often use the mean arterial pressure - cerebral blood flow (MAP-CBF) diagram to represent this phenomenon.

According to the original theoretical cerebral autoregulation curve, for a MAP value between 60 and 150 mmHg (the lower and upper limit of autoregulation), CBF remains almost constant as shown by Figure 1. This theory was described by Lassen in 1959. The classic autoregulation curve was later rejected. The updated autoregulation curve has a similar shape, but its width is different. Recent studies suggest that the plateau is much narrower, around $5-10$ mmHg. It is also unclear whether the autoregulation curve is symmetric, as the brain might respond better to an increase in MAP than to a decrease. Obtaining the real curve is challenging, as measuring CBF has its own difficulties. Two common methods, Doppler ultrasound and magnetic resonance imaging, both have considerable measurement uncertainties [4], [5].

1.1. The myogenic response

The myogenic response is observed in arterioles that supply blood to the brain and heart, among other organs. It works as follows: when blood pressure increases, the vessel wall initially expands. If the pressure remains constant, the vessel then contracts, often to a diameter smaller than its original size [6]. This contraction increases blood flow velocity and decreases pressure. The vascular resistance of vessels depends heavily on their diameter ($R \sim \frac{1}{d^4}$), so

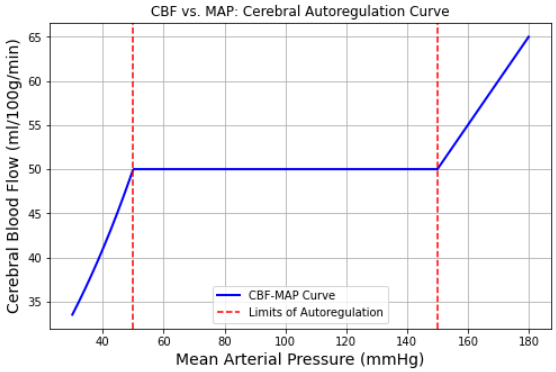

Figure 1. The original CBF-MAP curve.

by adjusting the diameter based on pressure, the body can regulate blood flow distribution to tissues and capillary pressure. Increased and maintained pressure in resistance arteries and arterioles causes these vessels to contract, a phenomenon known as the myogenic response. The steady-state response of these vessels is called myogenic tone. These mechanisms contribute to the autoregulation of blood flow in the brain, heart, skeletal muscles, and other organs [6].

Despite their importance, not all aspects of these biological functions are fully understood due to their complexity. Processes involving G-protein coupled receptors and ion channels, among others, play a role in the development of myogenic tone and response. The goal of mathematical modelling is not to encompass the entire process but focuses on establishing a direct relationship between pressure and peripheral resistance based on documented observations by physicians [6]. Mathematical models for myogenic autoregulation already exists in the literature [7], [8].

1.2. The metabolic response

Cells use Adenosine triphosphate (ATP) as a source of energy. ATP is typically produced through either oxidative phosphorylation or glycolysis, with the body preferring the former, which requires O_2. For this reason the body is in continuous need for O_2. O_2 demand can change for various reasons, including the onset of exercise. If the O_2 supply is insufficient, meaning that it does not match the need of the tissues, adenosine is produced. Adenosine, along with other substances produced as metabolic waste, causes vasodilation. Therefore, if the O_2 concentration is lower than needed, the vessels dilate, reducing their vascular resistance and allowing a larger blood flow to the tissue, increasing the O_2 supply. Literature suggests that the surface area responsible for O_2 diffusion also increases during exercise, increasing the amount of O_2 that can diffuse from the plasma to the tissues. This process results in a balance between the new level of O_2 demand and supply [1] [3].

The paper presents a comprehensive approach to simulate myogenic and metabolic blood flow regula-

tion, integrating insights from both literature research and mathematical modeling. The main objective of this work is to develop first_blood, a zero- and one-dimensional hemodynamic solver [2]. Researches regarding the control mechanisms could have real-world impact on medical research and clinical practice in the future. By advancing our ability to simulate these processes, it may pave the way for better diagnostic methods, targeted therapies, and new treatments for vascular disorders. The results of the simulations are thoroughly evaluated and discussed in the context of existing knowledge. The findings suggest that the simulations can mimic the behavior of the control mechanisms discussed, the myogenic and metabolic response models provide qualitatively correct results.

2. METHODS

2.1. Classic hemodynamic model

The model consists of large vessels modeled as axisymmetric tubes in one dimension (1D), which build up a vascular tree. The geometrical parameters (for example, diameter and length values) are taken from [9]. The vessels are elastic, and the relationship between the vessel deformation and the pressure described by a nonlinear function [10]. This, in addition to two fluid mechanics equations (the one dimensional mass and momentum equations) are solved with the method of characteristics and the MacCormack scheme [11]. Some parts of the cardiovascular system are modelled in zero dimension (0D) using electrical elements, e.g. resistors, inductors, capacitors, diodes and elastances. The smaller vessels (arterioles, capillaries and venules) and the veins are modelled using lumped models also, each compartment is taken into account with an RLC circuit at each periphery [12, 13]. The equations are solved the in-house hemodynamic solver, called first_blood [2].

2.2. Modeling the myogenic response

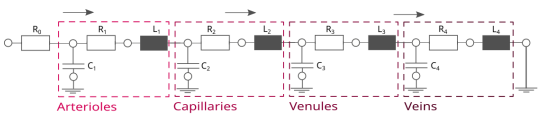

Figure 2. Peripheral models. Each compartment (arterioles, capillaries, venulares and veins) is modeled with an RLC circuit [12].

The simulation models the behavior of arterioles by considering the parameters of the peripheral models varying. For example, resistances vary with geometry, i.e., a smaller diameter results in higher resistance. In this context, the goal is to establish a relationship between peripheral resistances and pressure, since the myogenic response reacts to changes in blood pressure. First, an idealized relationship between pressure and peripheral resistance is given, based on a few assumptions:

- The arterioles are modeled as thick-walled tubes, since the ratio of the inner radius and the wall thickness is around $\frac{3}{4}$ [14].
- Since the Poisson coefficient of the vessel walls is close to 0.5 [2], it is an acceptable approximation to consider it incompressible.
- The shortening of the vessels as a response to increased pressure is neglected. Combining this with incompressible wall means constant area for the annulus.
- Theoretically the vessels response to stretch, trying to maintain constant circumferential wall tension despite changes in pressure [1]. We assume that the body strives to keep the circumferential wall tension constant at the inner diameter of the vessel.
- The pressure outside the arterioles is atmospheric.

The circumferential wall tension for a thick walled-tube can be written as:

$$\sigma_\theta(u) = \frac{pa^2}{b^2 - a^2}\Big(1 + \frac{b^2}{u^2}\Big), \tag{1}$$

where a and b are the inner and outer radius of the tube, p is the internal pressure and u is the radial coordinate ($a \leq u \leq b$). The third assumption above can be written in mathematical form:

$$(r + h)^2 - r^2 = c, \tag{2}$$

where c is a constant parameter, h is the wall thickness and r is the inner radius of the annulus. h can be determined as a function of r as $h = -r \pm \sqrt{r^2 + c}$ from Eq. (2). Since h, r and c are all positive, $h = -r + \sqrt{r^2 + c}$.

From the fourth assumption Eq. (1) should be evaluated at $u = r$. The inner radius of the tube is naturally $a = r$. We obtain:

$$\sigma_{\theta,0} = \frac{pr^2}{b^2 - r^2}\Big(1 + \frac{b^2}{r^2}\Big), \tag{3}$$

where $\sigma_{\theta,0}$ is constant. Substituting $b = r + h$ and $h = -r + \sqrt{r^2 + c}$ to Eq. (3) we get:

$$\sigma_{\theta,0} = p\Big(1 + \frac{2r^2}{c}\Big). \tag{4}$$

As previously mentioned a relationship between the peripheral resistances (R) and the pressure is needed, making the peripheral parametes time-dependent. The resistances are inversely proportional to r^4, so

$$R = \frac{\left(\frac{\sigma_{\theta,0}}{p} - 1\right)^{-2}}{k}. \tag{5}$$

Note that k is a constant parameter. After dividing both sides with the nominal resistance we obtain:

$$R_{fact} = \frac{\left(\frac{\sigma_{\theta,0}}{p} - 1\right)^{-2}}{k^*}, \tag{6}$$

where k^* is also a constant parameter, and R_{fact} is a scaling factor of the nominal resistance. To determine the two constants ($\sigma_{\theta,0}$ and k^*) two equations are needed. $\sigma_{\theta,0}$ can be calculated by substituting $b = r + h$ to Eq. (3), rearranging and using the first assumption ($\frac{h}{r} \approx \frac{4}{3}$ if $p = p_{ref}$).

$$\sigma_{\theta,0} = p\Big(1 + \frac{2}{2\frac{h}{r} + (\frac{h}{r})^2}\Big) = \frac{29}{20} p_{ref} \tag{7}$$

This provides a value for $\sigma_{\theta,0}$, since p_{ref} is a given parameter from the reference model. k^* can be calculated by substituting the value of $\sigma_{\theta,0}$ to Eq. (6), since R_{fact} is 1 if $p = p_{ref}$. This gives $k^* = (\frac{29}{20} - 1)^{-2} = \frac{400}{81}$[1]. At this stage the theoretical idealised curve is given with all it's parameters and constants.

In reality the vessels can not expand or contract without limitations, meaning that function given by Eq. (6) is not realistic. Instead, we assume that the system aims to follow the derived curve but fails. A more realistic sigmoidal connection is assumed between the pressure and the scaling factor of R:

$$R_{fact} = \frac{R_{max} + R_{min} e^{-f \cdot x_{myo}}}{1 + e^{-f \cdot x_{myo}}}, \tag{8}$$

Eq. (6) and Eq. (8) are obviously really different functions. So the next step is to determine the parameters (R_{max}, R_{min} and f) of the sigmoid curve considering the derived curve given by Eq. (6). The applied method sets the parameters so that Eq. (8) approximates the saturation values at roughly the same points as Eq. (6).

For the slope fitting we have to give the value of f. By matching the derivatives of Eq. (8) and Eq. (6) at p_{ref} we get: $f = \frac{8}{R_{max} - R_{min}} \frac{\sigma_{\theta,0}}{p_{ref}^2 k^*} \left(\frac{\sigma_{\theta,0}}{p_{ref}} - 1\right)^{-3}$.

Since the vascular resistance is a function of the diameter, the saturation values can be given with the normalized diameters obtained from [15]. With $sat_{max} = 1.773$ and $sat_{min} = 0.772$, R_{min} and R_{max} can be determined as:

$$R_{min} = \begin{cases} sat_{min}, & \text{if } x_{myo} < 0 \\ 2 - sat_{max}, & \text{otherwise.} \end{cases} \tag{9}$$

$$R_{max} = \begin{cases} 2 - sat_{min}, & \text{if } x_{myo} > 0 \\ sat_{max}, & \text{otherwise.} \end{cases} \tag{10}$$

x_{myo}, the independent variable of the myogenic control can be calculated from p with a low-pass filter. The differential equation for the filter is [7],

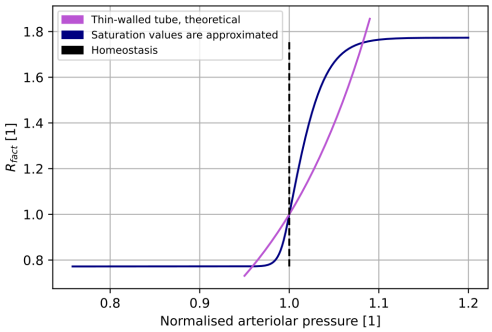

Figure 3. The theoretical curve given by 6 and the more resalistic sigmoidal curve.

$$\tau_{myo} \frac{dx_{myo}}{dt} = -x_{myo} + G_{myo}(\bar{p} - p_{ref}) \tag{11}$$

$G_{myo} = 0.9$ is the static gain, $\tau_{myo} = 40s$ is the time constant of the low-pass filter, $\bar{p}$ is the time-average of the last cardiac cycle and p_{ref} is the reference pressure. For each periphery p_{ref} is determined as the time average of the arteriolar pressure of the last cardiac cycle from a previous simulation (without any autoregulation). The simulation can calculate the scaling factor of resistances (R_{fact}) from the reference and the actual pressure with the given model. The arteriolar resistances are given for the next time step.

2.3. Modeling the metabolic control

Similar to the myogenic control, a sigmoidal connection between tissue O_2 level and the peripheral resistances is assumed. The saturation levels of the sigmoid curve are the same as for the myogenic control since the same vessels are responsible for these mechanisms and there is no information in the literature to suggest otherwise according to the author's knowledge. Similarly to the modelling of the myogenic response, the base simulation without any regulation mechanisms is used as the reference. Based on Eq. (8), the time dependent peripheral resistances can be determined as

$$R_{fact} = \frac{R_{max} + R_{min} e^{-f_{met} \cdot x_{met}}}{1 + e^{-f_{met} \cdot x_{met}}} \tag{12}$$

where f_{met} is scaled, so that the relative central slope is the same as in Eq. (8). The independent variable of the metabolic control (x_{met}) is calculate from C_t with a low-pass filter:

$$\tau_{met} \frac{dx_{met}}{dt} = -x_{met} + G_{met}(\bar{C}_t - \bar{C}_{t,ref}) \tag{13}$$

$G_{met} = 0.9$ is the static gain, $\tau_{met} = 40s$ is the time constant of the low-pass filter and $\bar{C}_t$ is the time average of C_t in the last cardiac cycle. For each periphery $\bar{C}_{t,ref}$ is calculated as the time average of the tissue O_2 concentration of the last cardiac cycle from

a previous simulation (without any autoregulation).

3. RESULTS AND DISCUSSION

3.1. Results of the myogenic response

Figure Figure (4) shows the simulated CBF-MAP curves with and without the myogenic response for the cerebral peripheries (the myogenic response for other peripheries were turned off for all simulations). The MAP values where modified by changing the miniumun of the elastance function of the left ventricle in the heart model that mimics the contraction of the heart. MAP was calculated as the time-average of the aortic pressure, CBF (the time-averaged volumetric flow rate of blood through the arteries supplying the intracranial system) is relative to the simulation computed with the base model.

A third-degree polynomial was fitted to the data points in both cases, since this type of function is recommended by physicians to describe autoregulation [16]. As expected, the myogenic response makes the CBF-MAP curve flatter over a certain range. However, the simulated curve is not as flat as the theoretical CBF-MAP curve, which is usually depicted with a more horizontal plateau. The simulation successfully mimics the body's behavior, meaning it attempts to maintain constant blood flow under varying conditions.

The myogenic mechanism responds to changes in blood pressure, but the body has multiple mechanisms that regulate blood pressure, e.g., the baroreflex. This means that the CBF-MAP curve observed by physicians is influenced by numerous factors [17]. Without accounting for these other processes, the simulated CBF-MAP curve cannot match the one measured in humans. It is also impossible to measure the effect of only the myogenic response in humans, since the other responses cannot be turned on or off independently.

Moreover, there are fairly different CBF-MAP curves found in the literature. The uncertanities of the CBF measurement methods (for example magnetic resonance imaging and transcranial Doppler ultrasound) are high [5], meaning that, achieving accurate numerical data is challenging, and the measurement error accumulates to the MAP-CBF curve. Since the model gives qualitatively correct results the model is found to be acceptable. In-vivo measurements could give the opportunity to calibrate the model to a for a population stochastically, or even a patient-specific level.

3.2. Results of the metabolic response

The metabolic response can be observed when an organ's O_2 demand increases, such as during exercise. The body responds by dilating resistance vessels, which increases blood flow to the organ. The increased O_2 demand can be modeled by changing the O_2 consumption term in the equations. To test whether the metabolic response model accurately mimics the body's behavior, four simulations

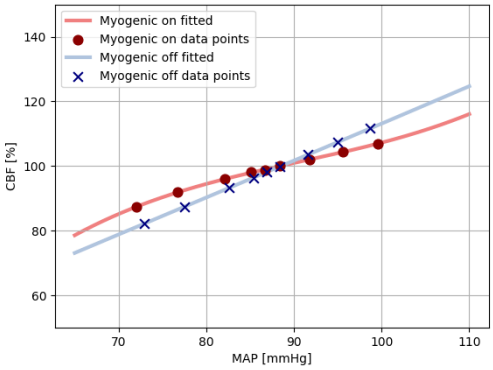

Figure 4. Evaluated CBF-MAP curves of the simulations. The myogenic response is only applied for the cerebral peripherals. The MAP values are modified by changing the miniumun of the elastance function of the left ventricle in the heart model that mimics the contraction of the heart. MAP is calculated as the time-average of the aortic pressure, CBF is relative to the simulation computed with the base model.

are computed. First, regulation is turned off, and all model parameters are set to their default values. In the second scenario, regulation is turned on, but the parameters remain the same. In the third scenario, the maximum oxygen consumption rate is doubled, but the metabolic response is turned off. In the fourth scenario is still doubled, but this time, the metabolic response is turned on. Overall every scenario is considered with the metabolic response and the modelled exercise.

The results of these simulations are shown in Figure (5). In the first two scenarios, the tissue O_2 concentration, the tissue oxygenation stabilizes at the same level, as expected. However, when O_2 consumption increases (in the third scenario), the tissue oxygenation decreases. When the metabolic response is activated (in the fourth scenario), the oxygenation increases and stabilizes between the values from the first two and the third scenarios. These results are consistent with expectations. The increased metabolic demand is regulated by increasing the diameters of the arterioles; thus, the blood flow is increased. The elevated blood flow tries to compensate the increased demand of O_2 in the tissues.

The model gives qualitatively accurate simulation results. The limitation of the study is the available in-vivo measurements. Performing in-vivo measurement on real patients requires both physicians with ethical approval, and expensive measurement setup. Moreover, the available measurement scenarios are highly limited, only certain variables can be measured directly, and only at certain locations. However, the main objective of future research is to collaborate with physicians and to obtain in-vivo

measurement data. Such data gives the opportunity to calibrate the model population- or even patient-wise.

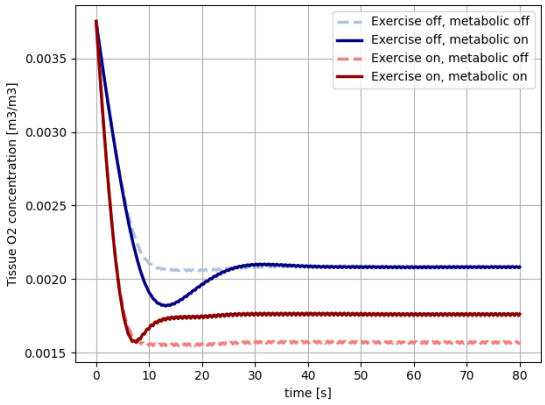

Figure 5. Evaluated CBF-MAP curves of the simulations. The myogenic response was only applied for the cerebral peripherals. The MAP values where modified by changing the minimun of the elastance function of the left ventricle in the heart model that mimics the contraction of the heart. MAP was calculated as the time-average of the aortic pressure, CBF is relative to the simulation computed with the base model.

3.3. Conclusion

The study presented a possible way to model two cardiovascular system control mechanisms, the myogenic and the metabolic response. Although both work locally, the myogenic response aims to ensure the constant circumferential shear stress, and to keep the blood flow constant and protect the vessels from overpressure. Traditional fluid and solid mechanical considerations determine a theoretical function for the pressure - peripheral resistance; however, lower and upper diameter boundaries limit the deformation keeping the physiological relevance. The metabolic response maintain the oxygen saturation level high ensuring the proper function of tissues and organs. The applied mathematical model builds on the same foundations as the myogenic one.

The simulation results suits the physiological relevance and gives qualitatively correct values. The myogenic model mimics the autoregulation, i.e., limits the effect of increased mean arterial pressure to the cerebral blood flow keeping the nutrient supply high despite changing physiological state. Analysing the metabolic response, by creating simulation scenarios with mimicking exercise by an increased oxygen demand could prove the qualitative relevance of the model. The results clearly set the direction for further research: in-vivo measurement can increase the validity of the models.

REFERENCES

[1] Pittman, R. N., 2016, *Regulation of tissue oxygenation*, Morgan & Claypool, San Rafael, California, second edition edn., ISBN 978-1-61504-721-5, oCLC: 957008214.

[2] Wéber, R., Gyürki, D., and Paál, G., 2023, "First blood: An efficient, hybrid one- and zero-dimensional, modular hemodynamic solver", *International Journal for Numerical Methods in Biomedical Engineering*, Vol. 39 (5), p. e3701.

[3] Fonyó Attila, Ligeti Erzsébet, Kollai Márk, and Szűcs Géza, 2008, *Az orvosi élettan tankönyve*, Medicina, Budapest, 4., átdolg., bőv. kiad edn., ISBN 978-963-226-126-3, oCLC: 909502283.

[4] Vitt, J. R., Loper, N. E., and Mainali, S., 2023, "Multimodal and autoregulation monitoring in the neurointensive care unit", *Frontiers in Neurology*, Vol. 14, p. 1155986, URL `https://www.frontiersin.org/articles/10.3389/fneur.2023.1155986/full`.

[5] Jones-Muhammad, M., and Warrington, J. P., 2021, "Redefining the cerebral autoregulatory range of blood pressures: Not as wide as previously reported", *Physiological Reports*, Vol. 9 (17), p. e15006.

[6] Jackson, W. F., 2021, "Myogenic Tone in Peripheral Resistance Arteries and Arterioles: The Pressure Is On!", *Frontiers in Physiology*, Vol. 12, p. 699517, URL `https://www.frontiersin.org/articles/10.3389/fphys.2021.699517/full`.

[7] Toro, E. F., Celant, M., Zhang, Q., Contarino, C., Agarwal, N., Linninger, A., and Müller, L. O., 2022, "Cerebrospinal fluid dynamics coupled to the global circulation in holistic setting: Mathematical models, numerical methods and applications", *International Journal for Numerical Methods in Biomedical Engineering*, Vol. 38 (1), p. e3532.

[8] Ursino, M., and Giannessi, M., 2010, "A Model of Cerebrovascular Reactivity Including the Circle of Willis and Cortical Anastomoses", *Annals of Biomedical Engineering*, Vol. 38 (3), pp. 955–974, URL `http://link.springer.com/10.1007/s10439-010-9923-7`.

[9] Reymond, P., Merenda, F., Perren, F., Rüfenacht, D., and Stergiopulos, N., 2009, "Validation of a one-dimensional model of the systemic arterial tree", *American Journal of Physiology-Heart and Circulatory Physiology*, Vol. 297 (1), pp. H208–H222, URL `https://www.physiology.org/doi/10.1152/ajpheart.00037.2009`.

[10] Olufsen, M. S., 1999, "Structured tree outflow condition for blood flow in larger systemic arteries", *American Journal of Physiology-Heart and Circulatory Physiology*, Vol. 276 (1), pp. H257–H268, URL https://www.physiology.org/doi/10.1152/ajpheart.1999.276.1.H257.

[11] Wéber, R., Viharos, M., Gyürki, D., and Paál, G., 2024, "Improvement for the hemodynamic solver, First Blood, using the MacCormack scheme", *Biomechanica Hungarica*.

[12] Liang, F., Takagi, S., Himeno, R., and Liu, H., 2009, "Biomechanical characterization of ventricular–arterial coupling during aging: A multi-scale model study", *Journal of Biomechanics*, Vol. 42 (6), pp. 692–704, URL https://linkinghub.elsevier.com/retrieve/pii/S0021929009000268.

[13] Jones, G., Parr, J., Nithiarasu, P., and Pant, S., 2021, "A physiologically realistic virtual patient database for the study of arterial haemodynamics", *International Journal for Numerical Methods in Biomedical Engineering*, Vol. 37 (10), p. e3497.

[14] Müller, B., Lang, S., Dominietto, M., Rudin, M., Schulz, G., Deyhle, H., Germann, M., Pfeiffer, F., David, C., and Weitkamp, T., 2008, "High-resolution tomographic imaging of microvessels", San Diego, California, USA, p. 70780B, URL http://proceedings.spiedigitallibrary.org/proceeding.aspx?doi=10.1117/12.794157.

[15] Zhang, C., Rogers, P. A., Merkus, D., Muller-Delp, J. M., Tiefenbacher, C. P., Potter, B., Knudson, J. D., Rocic, P., and Chilian, W. M., "Regulation of Coronary Microvascular Resistance in Health and Disease", .

[16] Brassard, P., Labrecque, L., Smirl, J. D., Tymko, M. M., Caldwell, H. G., Hoiland, R. L., Lucas, S. J. E., Denault, A. Y., Couture, E. J., and Ainslie, P. N., 2021, "Losing the dogmatic view of cerebral autoregulation", *Physiological Reports*, Vol. 9 (15), URL https://onlinelibrary.wiley.com/doi/10.14814/phy2.14982.

[17] Tlałka, K., Saxton, H., Halliday, I., Xu, X., Taylor, D., Narracott, A., and Malawski, M., 2024, "Local Sensitivity Analysis of a Closed-Loop in Silico Model of the Human Baroregulation", L. Franco, C. De Mulatier, M. Paszynski, V. V. Krzhizhanovskaya, J. J. Dongarra, and P. M. A. Sloot (eds.), *Computational Science – ICCS 2024*, Vol. 14835, Springer Nature Switzerland, Cham, ISBN 978-3-031-63771-1 978-3-031-63772-8, pp. 173–187, URL https://link.springer.com/10.1007/978-3-031-63772-8_17, series Title: Lecture Notes in Computer Science.